Tethered Particle Motion Method for Studying Transcript Elongation by a Single RNA Polymerase Molecule

Hong Yin,* Robert Landick,‡ and Jeff Gelles§
*Biophysics Program, Department of Biochemistry, and §The Center for Complex Systems, Brandeis University, Waltham, Massachusetts 02254; and ‡Department of Biology,‡Washington University, St. Louis, Missouri 63130 USA

ABSTRACT Schafer et al. (*Nature 352*:444–448 (1991)) devised the tethered particle motion (TPM) method to detect directly the movement of single, isolated molecules of a processive nucleic acid polymerase along a template DNA molecule. In TPM studies, the polymerase molecule is immobilized on a glass surface, and a particle (e.g., a 0.23 μm diameter polystyrene bead) is attached to one end of the enzyme-bound DNA molecule. Time-resolved measurements of the DNA contour length between the particle and the immobilized enzyme (the "tether length") are made by determining the magnitude of the Brownian motion of the DNA-tethered particle using light microscopy and digital image processing. We report here improved sample preparation methods that permit TPM data collection on transcript elongation by the *Escherichia coli* RNA polymerase at rates ($\sim 10^2$-fold higher than those previously obtained) sufficient for practical use of microscopic kinetics techniques to analyze polymerase reaction mechanisms. In earlier TPM experiments, calculation of tether length from the observed Brownian motion was based on an untested numerical simulation of tethered bead Brownian motion. Using the improved methods, we have now empirically validated the TPM technique for tether lengths of 308–1915 base pairs (bp) using calibration specimens containing particles tethered by individual DNA molecules of known lengths. TPM analysis of such specimens yielded a linear calibration curve relating observed Brownian motion to tether length and allowed determination of the accuracy of the technique and measurement of how temporal bandwidth, tether length, and other experimental variables affect measurement precision. Under a standard set of experimental conditions (0.23 μm diameter bead, 0.23 Hz bandwidth, 23°), accuracy is 108 and 258 bp r.m.s. at tether lengths of 308 and 1915 bp, respectively. Precision improves linearly with decreasing tether length to an extrapolated instrumentation limit of 10 bp r.m.s. and improves proportionally to the inverse square root of measurement bandwidth (1.9×10^2 bp $Hz^{-1/2}$ for 1090-bp tethers). Measurements on large numbers of individual polymerase molecules reveal that time-averaged single-molecule elongation rates are more variable than is predicted from the random error in TPM measurements, demonstrating that the surface-immobilized RNA polymerase molecules are kinetically heterogeneous.

INTRODUCTION

The *Escherichia coli* RNA polymerase is a processive nucleic acid polymerase. During transcript elongation, a single enzyme molecule completes the synthesis of an entire product RNA up to several thousand nucleotides in length, with concomitant movement of the enzyme molecule along a template DNA molecule (Dunn and Studier, 1980; Yager and von Hippel, 1987). The enzyme can be viewed as a chemically powered molecular motor: it catalyzes a chemical reaction (addition of nucleotides to the end of the growing product strand) and uses some of the free energy liberated by this reaction to power directed mechanical movement of the polymerase along the template. Full understanding of the elongation mechanism requires knowledge of the mechanical steps by which the enzyme moves along the template and of the kinetic "rules" (Jencks, 1980) that couple these steps to the chemical reactions of nucleotide polymerization. Cells use regulation of transcript elongation and termination reactions as a means to control gene expression (reviewed in Kerppola and Kane, 1991, and Landick and Turnbough, 1992). A thorough knowledge of the mechanisms of these reactions is therefore needed to further our understanding of the molecular basis of gene control.

The mechanism of transcript elongation by *E. coli* RNA polymerase has been analyzed in several types of experiments. The kinetics of the reaction have been studied under a variety of conditions by measuring the steady-state rate of incorporation of nucleotides into RNA (Rhodes and Chamberlin, 1974; Schmidt and Chamberlin, 1984; Jin and Gross, 1991) and by examining the length distributions of RNA products after restarting elongation of stalled transcription complexes in transient-state experiments (Arndt and Chamberlin, 1990; Levin and Chamberlin, 1987; Levin et al., 1987). The pre-steady-state rapid-quench technique has also been used to study transcription elongation by the *E. coli* RNA polymerase (Erie et al., 1993; Wilson and von Hippel, 1994) and by the yeast RNA polymerase III (Matsuzaki et al., 1994). The results of these studies show that transcript elongation is a complex process. Measured elongation rates and the stability of the transcription complex vary profoundly with the template DNA sequence (Levin and Chamberlin, 1987; Arndt and Chamberlin, 1990; Krummel and Chamberlin, 1992a). Even when positioned at a single DNA sequence, different polymerase molecules in a population may exist in different, kinetically distinguishable states that do not rapidly interconvert (Erie et al., 1993), leading to the proposal of an elongation mechanism with multiple branched

Received for publication 30 August 1994 and in final form 19 September 1994.

Address reprint requests to Dr. Jeff Gelles, Department of Biochemistry, Brandeis University, Waltham, MA 02254-9110. Tel.: 617-736-2377, Fax: 617-736-2349; E-mail: gelles@ binah.cc.brandeis.edu.

0006-3495/94/12/2468/11 $2.00

pathways (Erie et al., 1992, 1993). Finally, there is evidence that at least a portion of the RNA polymerase molecule may move along the template in steps larger than a single base pair (bp) (Krummel and Chamberlin, 1992b; Nudler et al., 1994; Chamberlin, 1994; Chan and Landick, 1994); if this is the case, proposed mechanisms based on identical cycles of single nucleotide addition to the transcript may be incomplete. Each of these phenomena can lead to the simultaneous presence of multiple chemical states in populations of elongating transcription complexes. Consequently, they complicate the interpretation of conventional biochemical experiments, which are restricted to observing the population-averaged properties of a molecular ensemble.

To circumvent this problem, Schafer et al. (1991) devised a tethered particle motion (TPM) technique to observe the movement of single, isolated RNA polymerase molecules along template DNA during transcript elongation. In a TPM experiment, stalled ternary transcription complexes (Levin et al., 1987), containing an RNA polymerase molecule in association with a template DNA and a nascent RNA transcript, are immobilized on a glass surface. One end of the template is labeled by a microscopic particle (e.g., a 40 nm diameter colloidal gold particle) visible by differential interference contrast (DIC) light microscopy. The segment of DNA between the particle and the surface-immobilized polymerase molecule functions as a flexible tether that constrains particle Brownian motion to a small, approximately hemispherical region above the glass surface. Movement of the polymerase along the DNA during transcript elongation changes the length of the tether and therefore produces a change in the spatial extent of particle Brownian motion. This change in particle motion is measured with nanometer-scale precision using digital image processing techniques that determine the size of the motion-blurred particle image in time-averaged light microscope video recordings. Because the TPM technique detects the elongation reaction in a single molecule, it can in principle be used to analyze enzyme reaction mechanisms by the microscopic kinetics techniques developed to analyze conductance recordings from single transmembrane ion channels (Colquhoun and Hawkes, 1983; Moczydlowski, 1986). The TPM experiments detect reaction steps that translocate the polymerase along the template but not those that make and break covalent bonds in the RNA and nucleoside triphosphates. TPM method is thus complementary to conventional kinetics experiments, which detect bond making/breaking but do not directly observe translocation.

Schafer et al. (1991) demonstrated that the TPM method can be used to detect transcript elongation in single RNA polymerase molecules. However, because the yield of particle-labeled immobilized transcription complexes was low, they were unable to obtain TPM data in the quantity required for statistical analysis of single-molecule turnover rates. In the present work, we used modified transcription complex immobilization and particle-labeling techniques to increase the rate of TPM data collection by $\sim 10^2$-fold, allowing us to measure the distribution of steady-state elongation rates for single enzyme molecules. The increased data collection rate also allowed us to validate and calibrate the TPM method over a range of DNA tether lengths, to determine TPM measurement accuracy, and to analyze how TPM measurement precision is affected by a number of experimental variables.

MATERIALS AND METHODS

Chemicals

Nucleoside triphosphate stock solutions and D-biotin were purchased from Boehringer-Mannheim (Indianapolis, IN), ApU dinucleotide from Sigma Chemical Co. (St. Louis, MO), [α-^{32}P]GTP from Amersham (Arlington Heights, IL), and streptavidin from Molecular Probes (Eugene, OR). Avidin was obtained as an affinity-purified fraction (Avidin DN) from Vector Laboratories (Burlingame, CA). Conventional commercial avidin preparations proved unsuitable for use in TPM studies because they displayed high nonspecific binding to DNA (Fraenkel-Conrat et al., 1952). α-casein (Sigma Chemical Co.) stock solution was prepared at 5 mg ml^{-1} and then centrifuged at 34,540 $\times$ g for 10 min to remove insoluble material.

DNA templates

DNA templates for transcription reactions contained the strong *E. coli* RNA polymerase A1 promoter from phage T7 (Fig. 1). Templates were synthesized as described (Schafer et al., 1991), except that 35 cycles of polymerase chain reaction (PCR) were used. PCR templates and primers used for the construction of different transcription templates are listed in Table 1. To construct plasmid pRL572, a fragment of the *rpoB* gene was recovered as a *BamHI* to second *BclI* site (with *XhoI* linker) fragment of plasmid pRL385 (Landick et al., 1990) and was ligated to a *BamHI/SalI* fragment of pRL418 (Chan and Landick, 1989).

Avidin-coated beads

0.23 μm diameter carboxylated polystyrene microspheres ["beads"] (Polysciences Inc., Warrington, PA) were covalently biotinated, coated with avidin, and purified by gel filtration as described (Berliner, E., E. C. Young, K. Anderson, H. K. Mahtani, and J. Gelles, submitted for publication) except that dialysis and gel filtration buffers were bead buffer (20 mM Tris-acetate, pH 8.0, 130 mM NaCl, 4 mM $MgCl_2$, 0.1 mM EDTA). To minimize aggregation, bead preparations were used within 7 days of purification. Concentration of avidin-coated bead suspensions was measured as described (Berliner, E., E. C. Young, K. Anderson, H. K. Mahtani, and J. Gelles, submitted for publication).

Interaction of biotinated DNA with streptavidin or avidin

To measure the binding of biotinated DNA to biotin-binding proteins and the dissociation rates of the resultant complexes, we first prepared a biotinated, radiolabeled 1360-base pair (bp) double-stranded DNA using PCR

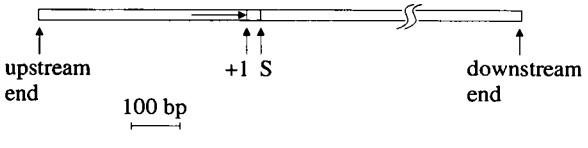

FIGURE 1 Structure of the transcription templates used in this study. (→) Phage T7 A1 promoter. (+1) Transcription start site. (S) Site at which transcription was stalled (Levin et al., 1987). The two ends of these linear double-stranded DNA molecules are designated "upstream" and "downstream" with respect to the orientation of the promoter.

TABLE 1 Transcription templates

Template	Parent plasmid*	Upstream primer‡	Downstream primer‡	Initial tether length (bp)§	Final tether length (bp)¶
572–1B-2	pRL572	PCR1B	PCR2	308	2148
185–1–3B	pCL185‖	PCR1	PCR3B	727	285
572–1–4B	pRL572	PCR1	PCR4B	1090	~0
572–1–5B	pRL572	PCR1	PCR5B	1620	~0
572–1–2B	pRL572	PCR1	PCR2B	1915	75

* Linearized plasmid used as PCR template (see Materials and Methods).
‡ Oligonucleotide primers used in the PCR reaction. Primers with a "B" suffix have a biotin moiety linked to the 5′ oxygen atom. Primers PCR1B, PCR2B, and PCR3B have the biotin moiety linked through a six-carbon spacer (biotin-dX reagent, Midland Certified Reagent, Midland, TX) to oligonucleotides with structures biotin-dX-5′-d[GTAAAACGACGGCCAGT]-3′ (PCR1B), biotin-dX-5′-d[GCTTCGCAACGTTCAAATCC]-3′ (PCR2B) and biotin-dX-5′-d[AACAGCTATGACCATG]-3′ (PCR3B). PCR1 and PCR2 have the same sequences as PCR1B and PCR2B, respectively, without the biotin moiety. (Primers PCR1, PCR1B, PCR2, and PCR2B are the same as those used previously (Schafer et al., 1991).) PCR4B and PCR5B (Genosys Biotechnologies Inc., The Woodlands, TX) have the structures biotin-spacer-5′-d[GGTTTCAGAGATATATGGGC]-3′ and biotin-spacer-5′-d[TTGTGCGTAATCTCAGACAG]-3′, respectively, where "spacer" represents —$NH(CH_2)_5CONH(CH_2)_5CONH(CH_2)_6OPO_3^-$—.
§ Length of the DNA segment between the biotin moiety and the transcriptional stalling site (Levin et al., 1987).
¶ Length of the DNA segment between the biotin moiety and the last transcribed nucleotide. Templates 572–1B-2 and 572–1–2B each have the strong *rrnB* T1 terminator 75 bp from the downstream end; template 185–1–3B has an *rrnB* T1 terminator 285 bp from the downstream end. Most RNA polymerase molecules transcribing these templates would terminate at *rrnB* T1. Other templates do not have a terminator at the downstream end, and the polymerase could therefore in principle transcribe to the end of the template.
‖ See Feng et al. (1994).

conditions and purification procedures described previously (L. Finzi and J. Gelles, submitted for publication). The PCR template was *Sca*I-linearized pRW490 (Hsieh et al., 1987) and the primers were 5′-biotin-dX-d-[AGATCCAGTTCGATGT]-3′ and 5′-d[CACGATGCGTCCGGCG]-3′ (Midland Certified Reagent, Midland, TX). 100 μl PCR reactions were supplemented with 10 μCi [α-^{32}P] dCTP (NEN Research Products, Boston, MA).

Binding of biotinated DNA to streptavidin (or avidin) was detected with a gel mobility shift assay (Fried and Crothers, 1984). Excess streptavidin was added to an *Ssp*I digest of 1360-bp DNA (see figure legend for concentrations) in 8.6 mM Tris-Cl$^-$, pH 7.9, 8.6 mM $MgCl_2$, 43 mM NaCl, 0.86 mM dithiothreitol (DTT) and incubated 30 min at 37°. In experiments to measure the dissociation rate of the protein-DNA complex, a saturating amount of biotin was added to a series of identical samples and each was then incubated at 37°C for varying lengths of time. In all experiments, samples were then loaded on a nondenaturing 8% (w/v) polyacrylamide gel (*bis*:acrylamide = 1:19) in 0.5 × TBE buffer (Sambrook et al., 1989). After electrophoresis, the gel was stained in ethidium bromide and bands corresponding to the complex of the biotinated 162-bp digest fragment with protein bound were excised and counted for radioactivity. To verify that binding was specific, we performed control experiments in which the streptavidin (or avidin) was presaturated with biotin before use.

Stalled transcription complexes

Stalled transcription complexes (Levin et al., 1987) were formed as described (Lee and Landick, 1992) with the following changes: complexes were formed at 37° for 20 min in a reaction mixture containing 20 mM Tris-Cl$^-$ pH 8.0, 20 mM NaCl, 14 mM $MgCl_2$, 0.1 mM EDTA, 14 mM 2-mercaptoethanol, 1.5% (w/v) glycerol, 250 μM ApU dinucleotide, 2.5 μM each ATP, GTP, and CTP, 0.2 μCi μl^{-1} [α-^{32}P]-GTP, 20 μg ml^{-1} acetylated bovine serum albumin (BSA), 15 μg ml^{-1} RNA polymerase, and 10 nM DNA template. The stalled complexes were then isolated on a gel filtration column (Lee and Landick, 1992) equilibrated with 130 mM KCl, 20 mM Tris-Cl$^-$, pH 8.0, 4 mM $MgCl_2$, 0.1 mM EDTA, 0.1 mM DTT, 20 μg ml^{-1} acetylated BSA, 4% (w/v) glycerol.

Preparation of samples for TPM measurements

Coverslip flow cells were prepared as described previously (Berliner et al., 1994) except that a rinse of the working surface with ethanol and H_2O was substituted for the acid treatment. Flow cells were ~0.1 mm thick with a volume of ~20 μl. Stalled transcription complexes diluted in PTC buffer (20 mM Tris-acetate, pH 8.0, 130 mM NaCl, 4 mM $MgCl_2$, 0.1 mM EDTA, 0.1 mM DTT, 20 μg ml^{-1} acetylated BSA, and 80 μg ml^{-1} heparin) were incubated in the flow cell at ~23°C for 20 min. The cell was then washed with 250 μl 5 mg ml^{-1} α-casein in PTC buffer to completely coat the glass surfaces with protein and to remove any transcription complexes not adsorbed to the glass. After 5 min incubation, the cell was further washed with 150 μl PTC buffer and then incubated for >30 min with avidin-coated beads in bead buffer supplemented with 1 mg ml^{-1} α-casein. Before microscope observation, free beads were washed from the cell with 400–500 μl final buffer (PTC buffer supplemented with 1 mg ml^{-1} α-casein and 1 mM biotin). Transcript elongation was started by flowing in 50 μl of 1 mM ribonucleoside triphosphates (NTPs) (i.e., 1 mM each of ATP, GTP, CTP, and UTP) in final buffer.

Surface density and active fraction of immobilized transcription complexes

To measure the surface density of radiolabeled transcription complexes on the flow-cell walls, flow cells were prepared as described for TPM samples except that the cell was dissembled after the PTC buffer washes. A measured area was cut from the flow cell wall and radioactivity eluted from the cut surface by 20% sodium dodecyl sulfate was counted. Transcription complex surface densities in excess of 10 μm^{-2} could be obtained, and surface densities were roughly proportional to the applied transcription complex solution concentration over a wide range (75 pM–1 nM) in agreement with results obtained previously (Schafer et al., 1991).

TPM experiments require specimens in which each bead is attached to only a single DNA molecule. However, because the avidin-coated beads may have multiple biotin binding sites, they have the potential to attach to multiple DNA molecules. To avoid this, we controlled the surface density (D) of transcription complexes on the flow-cell walls as previously described (Schafer et al., 1991). We assumed that the DNA templates of two immobilized complexes could not attach to the same bead unless $L \leq 2\,l + d$, where L is the distance between the two complexes, l is the initial tether length of the complexes (Table 1), and d is the bead diameter. The fraction (P) of immobilized complexes that have nearest neighbors such that $L \leq 2\,l + d$ is given by the Poisson distribution as:

$$P = 1 - \exp[-D\pi(2l + d)^2]. \quad (1)$$

In all reported TPM measurements, $P < 0.10$.

To measure the fraction of immobilized complexes that retain catalytic activity, flow cells were prepared as described for TPM samples through the PTC buffer wash step and then incubated 5–10 min at ~23° with 1 mM NTPs in PTC buffer. Radiolabeled transcripts were then eluted from the flow cell with 300 μl PTC buffer; the eluate was counted to determine the number of immobilized complexes that released their transcripts. This value was corrected (typically by 10–30%) for the number of transcripts released in otherwise identical control samples that lacked NTPs. The total number of immobilized complexes in the flow cell was calculated from the measured complex surface density and the total area of the flow-cell walls.

TPM data collection and image processing

Observation of the tethered beads by video-enhanced DIC light microscopy, and image recording and processing were as previously described (Schafer et al., 1991) with the exceptions noted. Except where noted, TPM image acquisition time was 4.3 s (128 video frames each 33.3 ms in duration). In some experiments, images were directly transferred to the digital storage device without first being recorded on videotape; the two methods yielded image size parameter values (Schafer et al., 1991) that differed by <3%. Except where otherwise indicated, the Brownian motion (δ) of a tethered bead was calculated as $\delta = S_T - \langle S_S \rangle$, where S_T and S_S represent image size parameters of a tethered and an immobile surface-attached bead in the same microscope field, and $\langle ... \rangle$ represents a time average over the duration of the video recording (L. Finzi and J. Gelles, submitted for publication).

Accuracy and precision of the TPM method

The accuracy of the TPM method was measured using beads tethered by transcription complexes in the absence of NTPs; such beads have a time-invariant tether length. Accuracy was calculated as the standard deviation of a set of δ values each obtained from a different bead.

To determine TPM measurement precision using samples with non-elongating transcription complexes, we first measured the variance (var(S)) of the image size parameter over 15 time points for each analyzed tethered bead. Precision was then calculated as $\overline{(\mathrm{var}(S))}^{1/2}$ where the line represents the average over the population of analyzed beads.

In some experiments to determine the effect of tether length on measurement precision, an alternative method was used to allow estimation of precision in populations of elongating transcription complexes. Data selected from the Brownian motion time course of an elongating transcription complex by a sliding window 48 s long was detrended by linear regression. The variance of the detrended data from each window was calculated, and the results from different transcription complexes were pooled and binned at intervals of 300 bp in tether length. Precision was calculated as the square root of the median value of the data in each bin.

To determine the effect of fixed background features in the microscope images on the tether length measurement, composite images were created by summing each bead image with six different background images taken from the same microscope field. The variance of the image size parameter (S) of the six summed images (var(S)) was calculated for nine immobilized and nine 1090-bp tethered beads. The effect of background features on the accuracy of the δ measurements was calculated as $(\overline{\mathrm{var}(S_T)} + \overline{\mathrm{var}(S_S)})^{1/2}$.

Elongation rates

Time-averaged single-complex elongation rates were determined by linear regression of δ versus time. Since measurement precision is poorer at longer tether lengths, only the first (for complexes with beads at the upstream template end) or last (for complexes with beads at the downstream template end) 72 s of elongation data were used to calculate elongation rates.

The variance in the rates measured this way was calculated as $\mathrm{var}(\delta) / \sum_{i=1}^{15} (t_i - \bar{t})^2$, where t_i are the time values for the 15 measurements of δ made within the 72-s interval and $\bar{t}$ is the mean of those values (Colquhoun, 1971). In calculations to estimate the intrinsic stochastic variability of single-molecule elongation rates, we used d^2t/τ_0 (where d is the single-turnover step size, τ_0 is the mean time interval between steps, and t is the 72-s data acquisition interval (Svoboda et al., 1994) as an estimated upper limit for the variance of the enzyme translocation distance.

RESULTS

Improvements to the TPM method

The TPM experiments reported here used the methods of Schafer et al. (1991), except that 1) a different protocol was used to immobilize the transcription complexes on the glass surface (see Materials and Methods), and 2) immobilized complexes were labeled with avidin-coated 0.23-μm polystyrene beads in place of the streptavidin-coated 40-nm colloidal gold particles used previously. These changes substantially increased the surface density of functional, particle-labeled immobilized transcription complexes, leading to greatly increased rates of TPM data acquisition.

In the modified TPM method, stalled transcription complexes were adsorbed to a treated glass surface, which was then washed with a buffer containing α-casein. Control experiments showed that adsorption to the surface under these conditions requires the presence of a transcription complex bound to the DNA; DNA alone does not bind appreciably. On average, 60 ± 17 (SD) % of the immobilized complexes were active as judged by the release of transcript from the surface in the presence of NTPs, similar to previous results (Schafer et al., 1991).

In the previous TPM study, the biotin-derivatized ends of template DNA molecules were labeled with streptavidin-coated colloidal gold particles. However, gel mobility shift assays demonstrate that the complex between streptavidin and the biotinated DNA derivative used here dissociates rapidly ($t_{0.5}$ < 5 min) in the presence of excess biotin. Therefore, most transcription complexes labeled with streptavidin-coated particles would not be expected to retain the particle for the duration of a TPM experiment (typically 10 min). In contrast, a purified avidin preparation (see Materials and Methods) formed kinetically stable complexes with the biotinated DNA. Dissociation of the avidin-DNA complex in the presence of excess biotin (Fig. 2) exhibited the biphasic kinetics typical of the dissociation of biotin derivatives from avidin (Garlick and Giese, 1988; Hofmann et al., 1982), with $t_{0.5}$ ~50 min. In addition, pretreatment of avidin with excess biotin before reaction with DNA reduced binding five- to seven-fold, indicating that the binding is largely specific. We

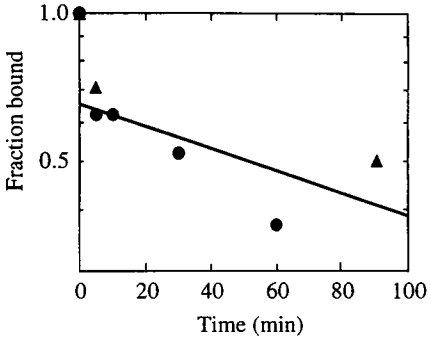

FIGURE 2 Dissociation time course of biotinated DNA-avidin complexes measured in a gel mobility shift assay. The dissociation reaction was initiated by adding excess competitor biotin (to final concentrations of 0.1 mM and 0.9 mM, respectively) to a mixture of 45 nM biotinated DNA fragment and 2.1 μM avidin (●), or 27 nM biotinated DNA and 1.7 μM avidin (▲). The plot shows the fraction (f) of DNA remaining bound to avidin at various times after addition of competitor, relative to the amount bound before competitor addition (logarithmic scale). (—) Least-squares fit of the function $f(t) = Ae^{-Kt}$ to the experimental data (excluding those at $t = 0$), yielding parameters $A = 0.66$, $k = 8.8 \times 10^{-5}$ s^{-1}.

therefore used avidin-coated particles in the modified TPM experiments. Microscopic polystyrene beads were used in place of the colloidal gold particles used previously because of the superior size uniformity and colloidal stability obtained with the beads (Morris and Saelinger, 1986). The dissociation of biotinated DNA from avidin-coated beads (data not shown) exhibits kinetics similar to those seen with free avidin.

In the earlier TPM study, transcription complexes designed to yield short initial tether lengths (e.g., complexes with template 572-1B-2 (Table 1)) were immobilized at a surface density of 0.6 μm^{-2}, but microscope observation revealed tethered particles at $<10^{-4}$ μm^{-2}. The apparent low efficiency with which immobilized complexes were labeled with particles, and the consequent scarcity of tethered particles observed in the microscope (much less than one tethered particle per video microscope field), made data collection extremely slow. This problem also made it impractical to collect TPM data on complexes with longer initial tether lengths (e.g., those made with downstream-biotinated templates (Table 1)) because the maximum complex surface density consistent with avoiding attachment of >1 DNA molecule/particle decreases dramatically with increasing initial tether length (Eq. 1). The modified TPM protocol used here greatly increases the efficiency with which immobilized transcription complexes are labeled with particles. At a complex surface density of 0.10 μm^{-2} (using template 572-1B-2), we now obtain tethered beads at 0.011–0.041 μm^{-2}, a labeling efficiency of 11–41%. Many tethered beads are routinely observed in a single video microscope field (441 μm^2), allowing simultaneous TPM data acquisition from a number of transcription complexes.

Calibration of the TPM method

To analyze transcript elongation quantitatively in a TPM experiment, it is necessary to know the relationship between the measured range of bead Brownian motion and the actual length of the DNA tether that links the bead to the surface.

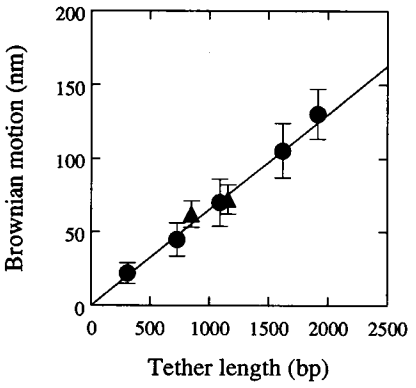

FIGURE 3 Brownian motion (mean ± SD) of 0.23 μm diameter avidin-coated beads tethered to a surface by known lengths of DNA. Brownian motion (δ') was calculated as $\delta' = (S_T - S_S)$, where S_T and S_S are the image size parameters (Schafer et al., 1991) of a tethered bead and an immobile surface-attached bead, respectively, in the same digitized microscope image. Each plotted point is derived from measurements on between 16 and 45 beads. (●) Template DNA attached at the transcriptional stalling site (Fig. 1) to surface-immobilized *E. coli* RNA polymerase. (▲) DNA (labeled at one end with digoxigenin) attached to surface-immobilized anti-digoxigenin IgG (data from L. Finzi and J. Gelles, submitted for publication). (—) Least-squares fit of data obtained with RNA polymerase attachment (fit line constrained to pass through the origin). Slope: 0.065 nm bp^{-1}

To produce a reliable calibration curve defining the relationship between these two quantities, TPM measurements were performed on complexes with different known initial tether lengths prior to restarting transcript elongation by the addition of NTPs (Fig. 3). To ensure that observed beads were in fact tethered to functional RNA polymerase molecules, we excluded data obtained from beads that did not exhibit transcript elongation upon subsequent addition of NTPs. Within experimental error, observed Brownian motion is proportional to tether length over the entire range of the tether lengths studied (308–1915 bp). These observations are consistent with the predictions of the numerical simulation of tethered particle Brownian motion reported previously (Schafer et al., 1991). In addition, beads attached to

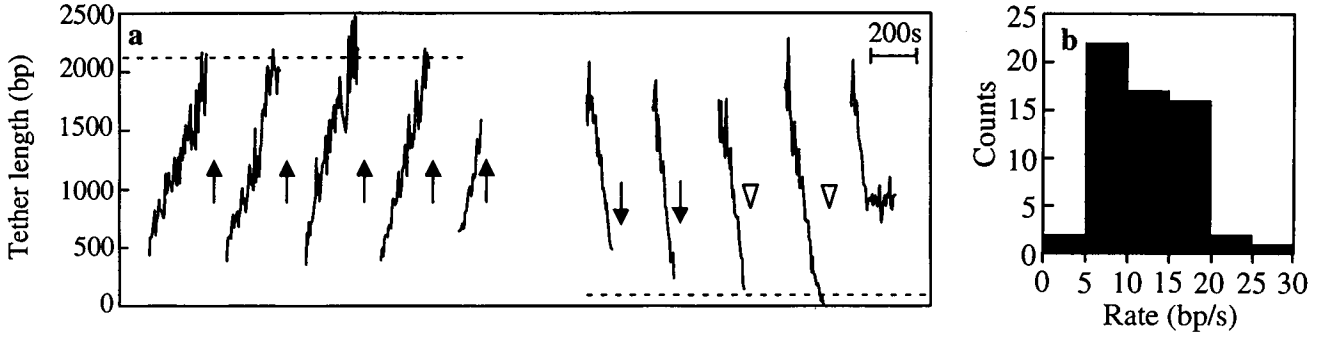

FIGURE 4 TPM measurements of transcript elongation by single RNA polymerase molecules at 1 mM NTPs, 23°. (*a*) Examples of tether-length time courses for immobilized transcription complexes labeled with beads at the upstream (traces 1–5, template 572-1B-2) or downstream (traces 6–10, template 572-1-2B) end of the template DNA molecule. (dashed lines) Expected final tether length. Release of the tethered bead from the glass surface (arrows) or spontaneous sticking of the tethered bead to the surface (triangles) occurred at the marked times. (*b*) Frequency distribution of the single complex elongation rates obtained from TPM measurements on 32 upstream-labeled (template 572-1B-2) and 28 downstream-labeled (equal numbers with templates 572-1-2B and 572-1-5B) transcription complexes.

DNA molecules linked to the glass surface by an alternative method (digoxigenin-labeled DNA linked to glass coated with anti-digoxigenin IgG (L. Finzi and J. Gelles, submitted for publication)) produced data that fell on the same calibration curve, suggesting that the details of DNA attachment to the surface do not alter the quantitative relationship between measured Brownian motion and tether length. The slope of the line fit to the calibration data (Fig. 3) was used to convert measured tethered bead Brownian motion to tether length in all subsequent experiments.

Transcript elongation rate distribution of single RNA polymerase molecules

The modified TPM method allowed us to observe single-molecule transcript elongation reactions in >460 immobilized transcription complexes labeled with beads at either the upstream or downstream end of the template (Fig. 4 *a*). The observed behavior of the upstream-labeled complexes is consistent with the limited data obtained previously; elongation of downstream-labeled complexes was not previously observed. In a sample of 60 single-molecule elongation reactions observed under identical conditions, most complexes (e.g., Fig. 4 *a*, traces 1–4 and 6–9) showed continuous elongation until their measured tether length was <500 bp from the expected final value (Table 1). This is consistent with studies of transcription complexes in solution that demonstrate that RNA polymerase is processive and that the majority of stalled transcripts can be chased into full-length products under elongation conditions similar to those used here (Lee and Landick, 1992). Most upstream-labeled complexes in this group ceased observable elongation when the tethered bead was released from the surface and diffused away (e.g., Fig. 4 *a*, traces 1–4). This is the behavior expected when the polymerase reaches the *rrnB* T1 terminator at the end of the template because the terminator triggers rapid dissociation of the template from the polymerase (Arndt and Chamberlin, 1988). Bead release was also observed with some downstream-labeled complexes (e.g., Fig. 4 *a*, traces 6 and 7); however, in the majority of such complexes the bead spontaneously stuck to the glass surface when the tether length became very short near the end of elongation (e.g., Fig. 4 *a*, traces 8 and 9). Only 14 of 60 complexes were observed to stop elongation prematurely. While some of these released the bead from the surface (Fig. 4 *a*, trace 5), others simply halted and thereafter maintained a constant tether length (Fig. 4 *a*, trace 10). The latter may correspond to the formation of "dead-end" complexes detected by analysis of the length distribution of RNA products from elongation reactions (Arndt and Chamberlin, 1990)

The single-molecule elongation rates of 60 complexes (32 upstream and 28 downstream labeled) exhibited a broad distribution (Fig. 4 *b*). The rate was 12.4 ± 4.9 (mean ± SD) bp s^{-1}, in agreement with results obtained in solution under similar conditions (13–20 bp s^{-1}; Schafer et al., 1991). Rates observed with upstream- and downstream-labeled complexes were similar (10 ± 3 and 15 ± 5 bp s^{-1}, respectively).

Precision and accuracy of TPM measurements

The overall accuracy of TPM measurements on elongating transcription complexes can be estimated by calculating the standard deviation of tether length measurements on the population of beads in the calibration samples, since each bead in these samples has the same nominal tether length. In such measurements under our standard experimental conditions, this quantity generally increases with tether length, ranging from 108 bp at 308-bp tether length to 287 bp at 1620-bp tether length (Fig. 3, error bars).

Factors that contribute to inaccuracy in TPM measurements can be grouped into two broad classes. The first class consists of noise sources that worsen measurement precision. These factors cause the variability observed when the TPM measurement is repeatedly performed on the same tethered bead under conditions (e.g., the absence of NTPs) in which the actual tether length is not changing. Factors that cause measurement imprecision include instrumentation noise and instability, as well as the statistical variation inherent in the measurement of the magnitude of a random process (the particle Brownian motion) in a finite time interval. The second class of factors that contribute to TPM measurement inaccuracy are those that cause additional variability of measurement results between members of a population of tethered beads. These factors account for the difference between estimates of measurement accuracy and measurement precision calculated as described above. Factors that cause population variability include those that cause variation in image magnification in different parts of the microscope field (e.g., geometric distortion in the camera or microscope optics).

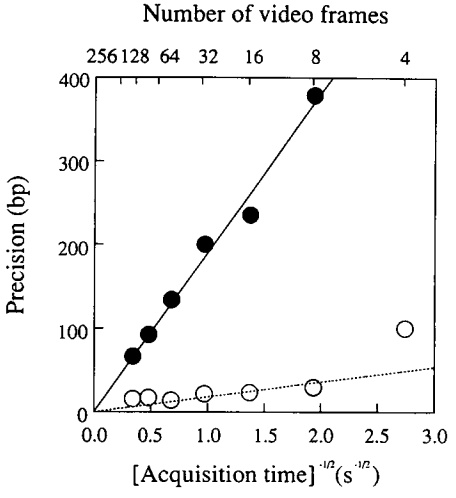

FIGURE 5 Effect of image acquisition time on TPM measurement precision. (●) Beads tethered by a 1090-bp DNA segment. (○) Immobile beads stuck to the glass surface. Precision is expressed as the square root of the time variance in tether length measurements; lower values mean better precision. Each microscope image for TPM analysis was prepared by averaging 4–256 consecutive 33.3-ms video frames, giving image acquisition times of 0.133–8.52 s. Each plotted point consists of combined precision measurements for 9 or 10 beads. (Solid, dotted lines) Linear least-squares fits (constrained to pass through the origin) of data excluding the point at four video frames averaging (see text). Slopes: 191 bp $Hz^{-1/2}$ (solid line) and 18 bp $Hz^{-1/2}$ (dotted line).

The most important experimental variable affecting measurement precision is the time used to acquire each microscope image, which dictates the temporal bandwidth of the measurement. As expected for a measurement containing bandwidth-limited noise (Bendat and Piersol, 1986), the precision of a TPM tether-length measurement is inversely proportional to the image acquisition time for acquisition times in the range 0.27–8.52 s (Fig. 5). Measurements on immobile beads had far better precision than those on tethered beads, indicating that most of the temporal variability in tether-length measurements arises from bead motion, not from instability of the microscope or image acquisition instrumentation. At the shortest image acquisition time (0.13 s; four video frames), sufficient data could not be collected from tethered beads, due to the failure of the curve-fitting algorithm (see Appendix) to converge. Inspection of the images revealed visibly asymmetrical bead shapes; this effect is expected because the short acquisition time is insufficient to allow bead Brownian motion to uniformly sample the space into which bead motion is constrained by the tether.

TPM measurements of elongating transcription complexes are visibly more noisy at the long tether length end of the trace than at the short tether length end (Fig. 4*a*). Several factors are expected to reduce measurement precision as the tether length increases. Longer tethers result in reduced contrast in bead images because the image is spread over a larger area and because the bead spends more time farther away from the microscope focal plane. Also, longer tethers increase the volume in which bead Brownian motion is constrained so that the sampling of that volume by bead movement during the image-acquisition time becomes less adequate. Experimental determinations of measurement precision by two methods confirm the predicted effect of tether length (Fig. 6). The r.m.s. variability in the tether length measurement increases by ~9 bp for every 100-bp increase in tether length over the range measured. The extrapolated precision at 0 tether length, 9.7 bp, agrees closely with the precision measured for immobile beads stuck to the glass surface. This suggests that the instrumentation limit on tether-length measurement precision at very short tether lengths is 9.7 bp under our standard experimental conditions (0.23 μm-diameter beads, image-acquisition time 4.3 s, 23°C).

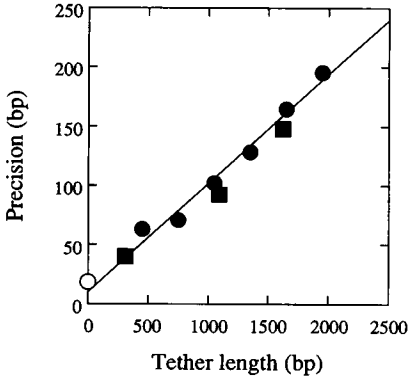

FIGURE 6 Effect of DNA tether length on TPM measurement precision at 4.3 s image-acquisition time; lower values mean better precision. (■, ●) Tethered beads. Precision was calculated from TPM measurements on beads tethered to non-elongating transcription complexes (■; 10 complexes for each plotted point), or on beads tethered to 32 elongating transcription complexes (template 572-1B-2) as described (●; see Materials and Methods). (Line) Fit line to elongating complex data with slope 0.092, intercept 9.7 bp. (○) Immobile beads stuck to the glass surface. Precision was calculated by the same method used for the elongating complexes (combined data from five beads).

As described earlier, the overall accuracy of the TPM measurement is worsened by factors that cause bead-to-bead variation in the measurement results. One such factor is the presence of fixed background features in the microscope images. Ideally, TPM measurements should be conducted on images of a tethered particle moving over a featureless background. In real experiments, the background is slightly irregular because of imperfections in the coverslip surface or microscope optics. The contribution of background features to TPM measurement variability was measured as 43 bp r.m.s. (see Materials and Methods) for 1090-bp tethers under standard conditions. This effect is small in comparison with the overall accuracy of 238 bp under these conditions (Fig. 3).

DISCUSSION

Improvements to the TPM method allow single-molecule kinetic analysis of transcription

The work presented demonstrates that TPM data can be collected and analyzed in sufficient quantity to allow statistical analysis of reaction kinetics in single enzyme molecules. It also demonstrates that the TPM method can reliably measure the length of DNA tethers in the size range 308–1915 bp and quantitatively evaluates the reproducibility and accuracy of the technique.

Relationship between measured bead Brownian motion and tether length

The empirical calibration curve (Fig. 3) shows that the tethered particle Brownian motion measured by the TPM technique is proportional to tether length for tethers of 308–1915 bp. In contrast, duplex DNA molecules in this size range conform closely to elastic chain models (Hagerman, 1988), and such models predict that the r.m.s. separation of chain ends increases less than proportionally to increasing contour length. (For DNA molecules in solution with contour lengths much greater than the persistence length, the models predict that r.m.s. end separation increases proportionally to the square root of the contour length. For the DNA molecules that tether beads to a glass surface in TPM preparations, this relationship may be altered by the excluded volumes of the bead and the surface.) However, TPM Brownian motion measurements do not simply reflect the r.m.s. end-to-end distance of the DNA tether. The microscope images used for the TPM measurements can be viewed as the convolution of

the spatial distribution of bead positions (projected into two dimensions) with the image of a stationary bead. The measured Brownian motion is the difference between the characteristic width of the resulting image and that of a stationary bead. Bead motion is constrained both by the DNA and by collision of the bead with the surface. In addition, the DNA is linked to the biotin moiety (and, therefore, to the bead) by a flexible aliphatic chain that should allow free movement of the bead center through a distance of up to one bead diameter (0.23 μm) about the DNA end. (This distance is of the same magnitude as the contour lengths of the DNA tethers used in this study.) Therefore, it is likely that the increase in observed Brownian motion as the tether is made longer is due to a reduction in the constraints to bead motion jointly imposed by the DNA, the aliphatic linker, and the glass surface, and not simply to a change in the distribution of DNA end positions. Consistent with this view, a simulation (Schafer et al., 1991) that did not consider duplex DNA stiffness or configurational entropy but simply treated the molecule as a flexible, inextensible string predicted a Brownian motion dependence on tether length essentially identical to that observed here.

Variance of single-enzyme transcription elongation rates

Measurement of elongation rates at saturating NTPs of individual RNA polymerase molecules revealed a rate distribution that was symmetrical within experimental error; the mean rate was 12.4 bp s^{-1}. The variance of the 60 single-molecule rate measurements was 24 bp^2 s^{-2} with a 90% confidence interval (assuming the rates are normally distributed) of 18–33 bp^2 s^{-2} (Mendenhall and Scheaffer, 1973).

Part of the observed overall width of the elongation rate distribution is due to the experimental uncertainty in the TPM tether length measurements from which the rates are calculated. The magnitude of the experimental uncertainty is given by the accuracy measurements (Fig. 3, error bars). As the tether length (and therefore the accuracy) changes during the course of the elongation rate measurement, we use the poorest accuracy value plotted in Fig. 3, which corresponds to 287 bp at 1620 bp tether length, to compute an estimated upper limit of 13 bp^2 s^{-2} on the contribution to the observed elongation rate variance from the uncertainty in TPM tether length measurements (see Materials and Methods).

A second factor that could contribute to the observed width of the elongation rate distribution is the inherent stochastic variability in the rates of single-molecule reactions. Such variability arises from the random nature of the thermal excitation that drives chemical reactions; it exists even when all molecules in the observed population have nominally identical structures and kinetic properties. Stochastic variability is maximum when only a single microscopic reaction step in the catalytic cycle limits the rate of enzymatic turnover (Svoboda et al., 1994). In that case, the number of steps made by a single molecule within a fixed time interval is Poisson distributed. However, assuming that RNA polymerase moves 1 bp along the template during each catalytic turnover, the maximum contribution to the variance in measured elongation rates from this source is 0.14 bp^2 s^{-2} which is negligible compared with the variance from the experimental uncertainty. Even if the enzyme moves in steps as large as 8 bp (Krummel and Chamberlin, 1992b; Nudler et al., 1994; see also Chamberlin, 1994; Chan and Landick, 1994), the stochastic variance is still minor (1.1 bp^2 s^{-2}).

Experimental uncertainty in the TPM measurements and the stochastic variability in single-molecule elongation rates together account for up to roughly half of the observed variance in the RNA polymerase elongation rates. The remaining variance can be attributed to kinetic differences from one transcription complex to the next. Factors that could contribute to this kinetic heterogeneity include: 1) DNA sequence dependence of elongation rates. Each elongation rate datum compiled in Fig. 4 b was obtained from 72 s of tether length measurements on a single transcription complex. However, we were not able to ensure that each polymerase molecule traversed exactly the same segment of template DNA sequence during that time period. This will contribute to variance in the observed elongation rates because, as previously discussed, elongation rates differ markedly at different template DNA sequences. This complication might be avoided in the future through the use of homopolymer templates. 2) Heterogeneity in the RNA polymerase preparation. The RNA polymerase preparation used in these studies is highly purified. Nevertheless, it is possible that the preparation contains subpopulations of molecules (e.g., due to posttranslational modifications) that have dissimilar kinetic properties, resulting in increased elongation rate variance in the population as a whole. Such kinetic heterogeneity is difficult to detect in conventional kinetic studies, which examine the population-averaged properties of molecular ensembles. 3) Heterogeneity due to surface attachment. The RNA polymerase molecules studied in these experiments are nonspecifically adsorbed to a glass surface. Surface-immobilized molecules may have different kinetic properties if they bind to the surface in different orientations or if their structures are altered in different ways by interaction with the surface. This surface-induced heterogeneity might be reduced or eliminated if a specific chemical linkage was used to attach the enzyme to the surface under conditions in which nonspecific adsorption does not occur. We have adopted this approach in studies on the microtubule-based mechanoenzyme kinesin (Berliner et al., 1994).

Accuracy and precision

The overall r.m.s. accuracy of the TPM technique was measured as 258 bp for a bead tethered by a 1915-bp DNA segment (4.3 s image-acquisition time). This corresponds to a relative error of 13%. The relative error increases substantially for shorter tethers. However, for many experiments it is the absolute error in the tether length measurements that is of primary concern. It is this quantity, for example, that affects the accuracy with which one can determine the

polymerase position relative to particular template sequence elements (e.g., terminators). Experiments that require absolute position measurements will work best with short tether lengths (Fig. 3), for which the absolute error is lowest (e.g., 108 bp at 308 bp tether length).

As previously described, inaccuracy in TPM measurements arises from both time-dependent and molecule-to-molecule variation in the measured tether lengths. Assuming that the two types of variation are statistically uncorrelated, the inaccuracy caused by the molecule-to-molecule variation alone can be calculated as $(A^2 - P^2)^{1/2}$ where A is the overall accuracy and P is the precision (Colquhoun, 1971). For 1090-bp tethers at 4.3 s image acquisition time, this quantity is 230 bp; molecule-to-molecule variation is therefore the major source of experimental error (the overall accuracy under these conditions is 248 bp). Only a small fraction of this variation can be explained by the measured variability due to fixed features in the bead image backgrounds (43 bp). The remainder must be attributed to heretofore unidentified sources of error. These might include factors (e.g., camera geometric distortion) that cause the imaging system point spread function to vary from position to position within the video microscope field (Inoue, 1986), or undetected transient sticking of some beads to the glass surface, resulting in an artifactually low Brownian motion measurement for those beads.

For some potential applications of the TPM technique, it is the precision of the method and not its accuracy that is the major determinant of experimental success. The reported experiments demonstrate that r.m.s. precisions of only a few tens of bp can be obtained under suitable conditions. The best precision obtained in this work was 40 bp r.m.s. measured for 308-bp tethers at 4.3 s image-acquisition time. Even better performance should be possible: the data of Figs. 5 and 6 suggest that precision can be further improved by reducing the tether length and also (at the expense of time resolution) by lengthening the image-acquisition time. Also, all reported accuracy and precision values are influenced to some extent by the signal-to-noise ratio of the pixel intensities in the TPM images. If this can be increased by improvements to the instrumentation, better precision and accuracy will likely result. Finally, alterations to the image shape function used to fit the TPM images (see Appendix) also can potentially improve the precision of TPM tether length data.

Other applications of the TPM method

The TPM method is a general technique to measure the contour length of a suitably bead-labeled and surface-immobilized DNA segment. As such, it can potentially be used in a wide variety of single-molecule kinetics experiments aside from the measurement of RNA polymerase elongation rates reported here. For example, the technique could be used to study enzymes other than RNA polymerase that move in a directed fashion along duplex DNA. These enzymes include a number of DNA helicases and DNA polymerases. In addition to studying enzyme movement per se, the technique can also be used to analyze control mechanisms that regulate the enzyme movement reactions. For example, TPM experiments could be used to directly examine the kinetics with which single RNA polymerase molecules exit from a transcriptional pause site (see Chan and Landick, 1994, for review). In a different kind of experiment, TPM techniques can be used to detect events that induce large configurational changes in single DNA molecules. For ex-

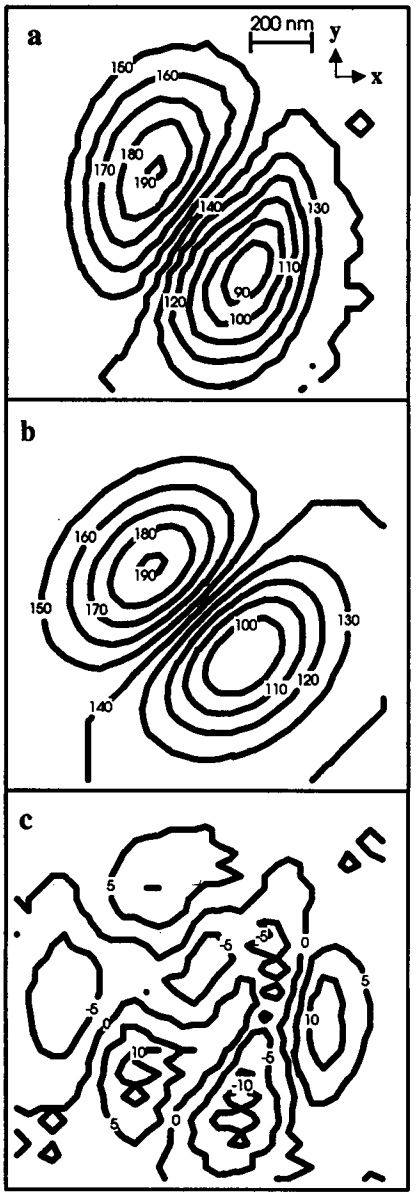

FIGURE 7 Computer fitting of a time-averaged (4.3 s) DIC microscope image of a 0.23 μm diameter bead tethered to the coverslip surface by a 1090-bp DNA segment. Pixel size: 41 nm. Plots display contours of equal light intensity (arbitrary units). The origin is at the upper left corner of each panel, with the positive x and y axes in the directions shown. (a) Experimental image. The image displays the apposed light (upper left) and dark (lower right) ovoids characteristic of a diffraction-limited DIC image. (b) Fit of Eq. A1 to the image in (a). Parameter values: S = 343 nm, h = 55.2, b = 141, x_c = 623 nm, y_c = 596 nm. Constants: α = 0.745, θ = 0.783 rad, ν = 0.767. (c) Fit residuals (experimental image in (a) minus fit image in (b)). Note reduced contour interval.

ample, (L. Finzi and J. Gelles, submitted for publication) tethered beads using a DNA containing two operator sites and used TPM methods to examine the kinetics of DNA loop formation and breakdown mediated by the *E. coli* lactose repressor protein. A similar approach might be used to study the kinetics of DNA interactions with other loop- or bend-inducing proteins. In summary, the advantages of the TPM approach are that it observes reactions of single protein and DNA molecules, not a molecular ensemble, and that it directly measures mechanistically relevant molecular movements. These attributes should prove helpful in elucidating reaction mechanisms in experimental systems of the types described.

APPENDIX: BEAD IMAGE ANALYSIS

The TPM method requires precise measurement of the size of motion-blurred, diffraction-limited DIC microscope bead images. This is accomplished by fitting the experimental images with a parameterized image shape function (Schafer et al., 1991). This function was empirically chosen to give a good fit to the experimental images. The function used is the difference of two two-dimensional Gaussians with their centers offset by a fixed distance (2ν) along the direction of the shear axis of the DIC microscope. The image light intensity (I) at the point (x,y) is given by:

$$I(x,y) = b + \frac{h}{e^{-4}-1}\left\{\exp\left[-\left(\frac{q}{S}\right)^2 - \left(\frac{p}{\alpha S} + \nu\right)^2\right] - \exp\left[-\left(\frac{q}{S}\right)^2 - \left(\frac{p}{\alpha S} - \nu\right)^2\right]\right\}$$

where $p = (x - x_c)\cos\theta - (y - y_c)\sin\theta$; $q = (x - x_c)\sin\theta + (y - y_c)\cos\theta$; S, h, b, x_c, and y_c are fitting parameters; and α, θ and ν are fixed constants that are determined by properties of the microscope imaging system. The fit parameters and constants have the following physical meanings: S is the image size parameter (Schafer et al., 1991) that reflects the width of the bead images. It is this parameter that is used to calculate the range of bead Brownian motion (see text). h is proportional to the difference in intensity between the brightest and darkest parts of the image. b is the uniform background light intensity at distances far from the bead center. (x_c, y_c) are the coordinants of the bead center. α is a dimensionless constant that adjusts the relative widths of the bead image in the directions parallel and perpendicular to the DIC microscope shear axis. θ is the angle between the shear axis and the image x axis. 2ν is the offset of the two Gaussians as described previously.

Eq. A1 was fit to the experimental images using a nonlinear least-squares program based on the Levenberg-Marquardt algorithm. (This requires numerical evaluation of Eq. A1 and its derivatives with respect to each of the parameters. A C language computer program that performs these calculations is available from the authors.) Fig. 7 shows an example of an experimental bead image and the fit of Eq. 1 to the image. Although the fit is generally good, the fit residuals (Fig. 7 *c*) show small but systematic deviations from 0. Therefore, it is possible that modifications to Eq. 1 could improve TPM measurement precision.

We thank Drs. Laura Finzi and Elise Berliner for sharing data and helpful discussions. Supported by grants from The Whitaker Foundation and the NIH (GM43369 and GM38660) and by Scholar Awards to J. G. from the Lucille P. Markey Charitable Trust and the Searle Scholars Program.

REFERENCES

Arndt, K. M., and M. J. Chamberlin. 1988. Transcription termination in *Escherichia coli:* measurement of the rate of enzyme release from rho-independent terminators. *J. Mol. Biol.* 202:271–285.

Arndt, K. M., and M. J. Chamberlin. 1990. RNA chain elongation by *Escherichia coli* RNA polymerase: factors affecting the stability of elongating ternary complexes. *J. Mol. Biol.* 213:79–108.

Bendat, J. S., and A. G. Piersol. 1986. Random Data. John Wiley and Sons, Inc., New York.

Berliner, E., H. K. Mahtani, S. Karki, L. F. Chu, J. E. Cronan, Jr., and J. Gelles. 1994. Microtubule movement by a biotinated kinesin bound to a streptavidin-coated surface. *J. Biol. Chem.* 269:8610–8615.

Chamberlin, M. J. 1994. New models for the mechanism of transcription elongation and its regulation. *In* The Harvey Lectures. Wiley-Liss, New York. 1–21.

Chan, C. L., and R. Landick. 1989. The *Salmonella typhimurium his* operon leader region contains an RNA hairpin-dependent transcription pause site. *J. Biol. Chem.* 264:20796–20804.

Chan, C. L., and R. Landick. 1994. New perspectives on RNA chain elongation and termination by *E. coli* RNA polymerase. *In* Transcription: Mechanism and Regulation. R. Conaway and J. Conaway, editors. Raven Press, New York, 297–320.

Colquhoun, D. 1971. Lectures on Biostatistics. Clarendon Press, Oxford.

Colquhoun, D., and A. G. Hawkes. 1983. The principles of the stochastic interpretation of ion-channel mechanisms. *In* Single-Channel Recording. B. Sakmann and E. Neher, editors. Plenum Press, New York. 135–175.

Dunn, J. J., and F. W. Studier. 1980. The transcription termination site at the end of the early region of bacteriophage T7 DNA. *Nucleic Acids Res.* 8:2119–2132.

Erie, D. A., O. Hajiseyedjavadi, M. C. Young, and P. H. von Hippel. 1993. Multiple RNA polymerase conformations and GreA: control of the fidelity of transcription. *Science.* 262:867–873.

Erie, D. A., T. D. Yager, and P. H. von Hippel. 1992. The single-nucleotide addition cycle in transcription: a biophysical and biochemical perspective. *Annu. Rev. Biophys. Biomol. Struct.* 21:379–415.

Feng, G., D. N. Lee, D. Wang, C. L. Chan, and R. Landick. 1994. GreA-induced transcript cleavage in transcription complexes containing *Escherichia coli* RNA polymerase is controlled by, multiple factors, including nascent transcript location and structure. *J. Biol. Chem.* 269: 22282–22294.

Fraenkel-Conrat, H., N. S. Snell, and E. D. Ducay. 1952. Avidin I. Isolation and characterization of the protein and nucleic acid. *Arch. Biophys. Biochem.* 39:80–96.

Fried, M. G., and D. M. Crothers. 1984. Kinetics and mechanism in the reaction of gene regulatory proteins with DNA. *J. Mol. Biol.* 172: 263–282.

Garlick, R. K., and R. W. Giese. 1988. Avidin binding of radiolabeled biotin derivatives. *J. Biol. Chem.* 263:210–215.

Hagerman, P. J. 1988. Flexibility of DNA. *Annu. Rev. Biophys. Biophys. Chem.* 17:265–286.

Hofmann, K., G. Titus, J. A. Montibeller, and F. M. Finn. 1982. Avidin binding of carboxyl-substituted biotin analogues. *Biochemistry.* 21: 978–984.

Hsieh, W.-T., P. A. Whitson, K. S. Matthews, and R. D. Wells. 1987. Influence of sequence and distance between two operators on interaction with the *lac* repressor. *J. Biol. Chem.* 262:14583–14591.

Inoue, S. 1986. Video Microscopy. Plenum Press, New York.

Jencks, W. P. 1980. The utilization of binding energy in coupled vectorial processes. *Adv. Enzymol.* 51:75–106.

Jin, D. J., and C. A. Gross. 1991. RpoB8, a rifampicin-resistant termination-proficient RNA polymerase, has an increased K_M for purine nucleotides during transcription elongation. *J. Biol. Chem.* 266:14478–14485.

Kerppola, T. K., and C. M. Kane. 1991. RNA polymerase: regulation of transcript elongation and termination. *FASEB J.* 5:2833–2842.

Krummel, B., and M. J. Chamberlin. 1992a. Structural analysis of ternary complexes of *Escherichia coli* RNA polymerase: individual complexes halted along different transcription units have distinct and unexpected biochemical properties. *J. Mol. Biol.* 225:221–237.

Krummel, B., and M. J. Chamberlin. 1992b. Structural analysis of ternary complexes of *Escherichia coli* RNA polymerase: deoxyribonuclease I footprinting of defined complexes. *J. Mol. Biol.* 225:239–250.

Landick, R., J. Stewart, and D. N. Lee. 1990. Amino acid changes in conserved regions of the β-subunit of *Escherichia coli* RNA polymerase alter transcription pausing and termination. *Gene Dev.* 4:1623–1636.

Landick, R., and C. L. Turnbough, Jr. 1992. Transcriptional attenuation. *In* Transcriptional Regulation. S. L. McKnight and K. R. Yamamoto, editors. Cold Spring Harbor Laboratory Press, Cold Spring Harbor, New York. 407–446.

Lee, D. N., and R. Landick. 1992. Structure of RNA and DNA chains in paused transcription complexes containing *Escherichia coli* RNA polymerase. *J. Mol. Biol.* 228:759–777.

Levin, J. R., and M. J. Chamberlin. 1987. Mapping and characterization of transcriptional pause sites in the early genetic region of bacteriophage T7. *J. Mol. Biol.* 196:61–84.

Levin, J. R., B. Krummel, and M. J. Chamberlin. 1987. Isolation and properties of transcribing ternary complexes of *Escherichia coli* RNA polymerase positioned at a single template base. *J. Mol. Biol.* 196:85–100.

Matsuzaki, H., G. A. Kassavetis, and E. P. Geiduschek. 1994. Analysis of RNA chain elongation and termination by *Saccharomyces cerevisiae* RNA polymerase III. *J. Mol. Biol.* 235:1173–1192.

Mendenhall, W., and R. L. Scheaffer. 1973. Mathematical statistics with applications. Duxbury Press, North Scituate, MA.

Moczydlowski, E. 1986. Single-channel enzymology. *In* Ion channel reconstitution. C. Miller, editor. Plenum Press, New York. 75–113.

Morris, R. E., and C. B. Saelinger. 1986. Problems in the production and use of 5 nm avidin-gold colloids. *J. Microsc.* 143:171–176.

Nudler, E., A. Goldfarb, and M. Kashlev. 1994. Discontinuous mechanism of transcription elongation. *Science.* 265:793–796.

Rhodes, G., and M. J. Chamberlin. 1974. Ribonucleic acid chain elongation by *Escherichia coli* ribonucleic acid polymerase. *J. Biol. Chem.* 249: 6675–6683.

Sambrook, J., E. F. Fritsch, and T. Maniatis. 1989. Molecular cloning: a laboratory manual. Cold Spring Harbor Laboratory Press, Cold Spring Harbor, NY.

Schafer, D. A., J. Gelles, M. P. Sheetz, and R. Landick. 1991. Transcription by single molecules of RNA polymerase observed by light microscopy. *Nature.* 352:444–448.

Schmidt, M. C., and M. J. Chamberlin. 1984. Amplification and isolation of *Escherichia coli nusA* protein and studies of its effects on in vitro RNA chain elongation. *Biochemistry.* 23:197–203.

Svoboda, K., P. P. Mitra, and S. M. Block. 1994. Fluctuation analysis of motor protein movement and single enzyme kinetics. *Proc. Natl. Acad. Sci. U.S.A.* In press.

Wilson, K. S., and P. H. von Hippel. 1994. Stability of *Escherichia coli* transcription complexes near an intrinsic terminator. *J. Mol. Biol.* In press.

Yager, T. D., and P. H. von Hippel. 1987. Transcript elongation and termination in *Escherichia coli.* In *Escherichia coli* and *Salmonella typhimurium:* Cellular and Molecular Biology. F. C. Neidhardt, J. L. Ingraham, B. Magasanik, K. B. Low, M. Schaechter, and H. E. Umbarger, editors. American Society for Microbiology, Washington, D.C. 1241–1275.